Invest in our future

Project Acronym: ISECA

Document Title: The TriOS processor to correct above water measurements for the sky-dome reflection

Version: 1.1

Author(s): F. Zagolski and R. Santer

Affiliation(s): ADRINORD, Association pour le Développement de la Recherche et de l'Innovation dans la Région Nord-Pas de Calais, Lille – France.

Modification History: First version, 31/01/12
Last version, 17/03/12

Distribution: ISECA Report

Executive summary: An alternative correction of the sky dome reflection is proposed to remove the reflection of the sea surface in the above water radiance measurements with the hyperspectral TriOS (Tri-Optical Sensors) instrument that were spectrally convoluted with the 13 MERIS filters (the 2 strong gaseous aborption bands being discarded from the MERIS bandset) upstream. This corrective method accounts for the polarized nature of the incident atmospheric light and of the *Fresnel* reflection of a wind-roughened sea surface. In order to perform this correction with in-situ measurements collected in the Northern sea (*i.e.*, over the Brittish channel) on an operational basis, the TriOS processor has been developed to use as inputs the original file of radiometric measurements provided by the MUMM (Management Unit of the North Sea Mathematical Models, Brussels - Belgium) institute and the associated aerosol parameters extracted from the MERIS Ocean-Aerosol product defined at the reduced resolution and available in MERMAID (MERis MAtchup In-situ Database). From the SEAPOL database, the MERIS look-up tables (LUTs) of upward/downward radiances pre-computed at bottom of the atmosphere (BOA) have been extracted for the TriOS view geometry. From these BOA radiance LUTs, a new *Fresnel* reflection coefficient is then deduced using as inputs the wind-speed value from the MERIS auxiliary data file and the atmospheric model observed with MERIS.

TABLE OF CONTENTS

LIST OF FIGURES

LIST OF TABLES

DOCUMENT CHANGE RECORD

Issue	*Rev.*	*Date*	*Chapter/Paragraph Number, Change Description (and Reasons)*
Draft	-	Jan. 31, 2012	- First draft of the document
1	0	Feb. 01, 2012	- Release of the first draft of the document
1	1	Mar. 17, 2012	- Full revision of the document

1. INTRODUCTION

1.1. Purpose of Document

In the validation of the algorithm for the MERIS (MEdium Resolution Imaging Spectrometer) atmospheric corrections over ocean, the water reflectance derived from in-situ measurements represents a key element. The database of above water radiometric measurements collected with the Tri-Optical Sensor (TriOS) [RD-1] over the Northern sea by the Management Unit of the North Sea Mathematical Models (MUMM, Brussels - Belgium) institute is particularly relevant for the validation strategy. The TriOS instrument combines simultaneous radiometric acquisitions of the direct solar irradiance at surface level, of the above water radiance and of the downwelling sky radiance. The water-leaving radiance needs to be corrected for the sky dome *Fresnel* reflection. In the standard protocol, this correction is completed without accounting for the polarization although the in-situ measurements are collected under geometric conditions favourable to the appearance of a significant polarization effect. The impact of neglecting the polarization has been fully illustrated in [AD-1] and a simulator (namely POLREF) has been developed [AD-2] to produce this new *Fresnel* reflection coefficient.

The main purpose of this document is to describe how to implement an alternative correction of the sky dome reflection accounting for the polarization in the TriOS data processing chain used at least by the MUMM institute to get the new water-leaving radiance to be reported in the MERis MAtchup In-situ Database (MERMAID) [RD-2].

1.2. Scope

This work is essential for the MERIS (MEdium Resolution Imaging Spectrometer) calibration and validation activities conducted for quality assurance of derived products over ocean including the collection of in-situ measurements for matchups with the spaceborne sensor.

1.3. Document Overview

Section 2 fully describes the TriOS processor and the approach used to achieve this new sky dome correction based on one data sample extracted from the full archive collected in Northern sea (i.e., over the Brittish channel). The original TriOS data file, provided by the MUMM institute, provides all the informations required to recompute the direct Sun glint contribution at bottom of the atmosphere (BOA). Using both the wind-speed value and the total ozone amount from European Centre for Medium range Weather Forecast (ECMWF), and the aerosol parameters (model, aerosol optical thickness and *Angstroem* exponent) extracted from the MERIS level-2 auxiliary data file (ADF), a new *Fresnel* reflection coefficient of the sea surface is then computed. At the end, the processor provides a new TriOS file with the water-leaving radiance corrected for both the reflected Sun glint at BOA and the sky dome *Fresnel* reflection, and with additional outputs (*i.e.*, the

reflected Sun glint radiance at BOA and the *Fresnel* reflection coefficient of the sea surface) for a quality control.

In Section 3 will be presented and analyzed the results of the new water-leaving radiances obtained for the full MUMM data archive. This section will be completed as soon as the whole set of TriOS data sequences will be processed at ARGANS Ltd (U.K.) with this new sky dome correction implemented in their own MERMAID processing chain.

Section **Error! Reference source not found.** will discuss how to generate the new water reflectances derived from TRIOS measurements from NIVA both during the MERIS matchups and on a systematic basis.

1.4. References

This section presents a list of applicable and reference documents.

1.4.1. Applicable documents

No	*Document*	*Title*
[AD-1]	*ATBD-Sky-Dome*	"Correction of the Water-leaving Radiance for the Fresnel Reflection of the Sky Dome accounting for the Polarization" – D1: ATBD report
[AD-2]	*POLREF-Simulator*	"Correction of the Water-leaving Radiance for the Fresnel Reflection of the Sky Dome accounting for the Polarization" – D2: POLREF report
[AD-3]	*CO-SCI-ARG-TN-0008*	"MERIS Optical Measurement Protocols – Part A: In-situ Water Reflectance Measurements"
[AD-4]	*SeaPRISM-Processor*	"Correction of the Water-leaving Radiance for the Fresnel Reflection of the Sky Dome accounting for the Polarization" – D3: SeaPRISM Processor report
[AD-5]	*PO-TN-MEL-GS-0002*	"MERIS Level-2 Detailed Processing Model & Parameter Data List"
[AD-6]	*PO-RS-PAR-GS-0002*	"Specification of the Scientific Contents of the MERIS Level-2 Auxiliary Data Products"

1.4.2. Reference documents

No	*Reference (authors, title, journal)*
[RD-1]	**Ruddick, K.G., V. De Cauwer, Y-J. Park, and G. Moore, 2006.** "Seaborne measurements of near-infrared water-leaving reflectance: The similarity spectrum for turbid waters", *Limnology Oceanography*, **51**(2): 1167-1179.
[RD-2]	**Barker, K., C. Mazeran, C. Lerebourg, M. Bouvet, D. Antoine, M. E. Ondrusek, G. Zibordi, and S. J. Lavender, 2008.** "MERMAID: The MERis MAtchup In-situ Database". In *ESA proceedings of 2nd MERIS (A)ATSR Users Workshop*, Frascati (Italy), Sept. 2008.

[RD-3] **Mobley, C.D., 1999.** "Estimation of the remote-sensing reflectance from above-surface measurements", *Applied Optics*, **38**: 7442–7455.

[RD-4] **Hansen, J.E., and L. Travis, 1974.** "Light scattering in planetary atmospheres", *Space Science Reviews*: **16**, 527-610.

[RD-5] **Shettle, E.P., and R.W. Fenn, 1979**. "Models for the aerosols of the lower atmosphere and the effects of humidity variations on their optical properties", *Air Force Geophysical Laboratory, Technical Report AFGL-TR-79-0214*, Hanscom Air Force Base (Mass.).

[RD-6] **Santer, R., and F. Zagolski, 2006**. "Inherent optical properties of the aerosols – IOPA", *in reponse to RFQ/3-11641/06/I-OL, Intended Rider 1 to ESRIN Contract 18109/04/I-OL for Atmospheric Correction for MERIS Over Coastal Waters: Towards a New Aerosol Climatology*: 40 p.

[RD-7] **Cox, C., and W. Munk, 1954.** "Measurements of roughness of the sea surface from photographs of Sun glitter", *Journal of Optical Society in America*, **44** (11): 838-888.

[RD-8] **Thuillier, G., M. Hersé, D. Labs, T. Foujols, W. Peetermans, D. Gillotay, P.C. Simon, and H. Mandel, 2003.** "The solar spectral irradiance from 200 to 2400 nm measured by the SOLSPEC spectrometer from the ATLAS and EUREKA missions", *Solar Physics,* **214:** 1–22.

[RD-9] **Santer R., F. Zagolski, and O. Aznay, 2010.** "Aerosol phase function derived from CIMEL measurements", *International Journal of Remote Sensing*, **31** (4): 969–992

1.5. Acronyms and abbreviations

1.5.1. Acronyms

ADRINORD	Association pour le Développement de la Recherche et de l'Innovation dand le NORD
ADF	Auxiliary Data File
AERONET	AErosol RObotic NETwork from NASA/GSFC (Greenbelt, MA)
AOT	Aerosol Optical Thickness
ARGANS	Applied Research in Geomatics, Atmosphere, Nature & Space (Plymouth, UK)
ATBD	Algorithm Theoretical Basis Document
BOA	Bottom Of the Atmosphere
CIMEL	In-situ radiometer used for collecting Sun extinction and sky radiance measurements
DPM	Detailed Processing Model
ECMWF	European Centre for Medium range Weather Forecast
FOV	Field Of View
LUT	Look-Up Table
IOP	Inherent Optical Property
IOPA	Inherent Optical Properties of the Aerosols
IPF	MERIS Instrument Processing Facility, successor of MEGS8.0 (Ground MERIS Ground Segment data processing prototype developed at ACRI-ST, Sophia-Antipolis, France.)
MERIS	MEdium Resolution Imaging Spectrometer
MERMAID	MERis Matchup In-situ Database
MUMM	Management Unit of the North Sea Mathematical Models institute (Brussels- Belgium)
OOT	Ozone Optical Thickness
POLREF	Simulator to compute the Fresnel POLarization REFlection coefficient of sea surface
RAA	Relative azimuthal angles (between Sun/view directions)
ROT	Rayleigh Optical Thickness

RPD	Relative Percentage Difference
RR	Reduced Resolution (mode used for MERIS data acquisition)
RTC	Radiative Transfer Code
SAA	Solar Azimuthal angle
SAM	Standard Aerosol Model
SEAPOL	Sea POLarization (project name or database name including *Stokes* parameters [I,Q,U] of BOA upward/downward radiance fields and downward transmittances)
SeaPRISM	SeaWiFS Photometer Revision for Incident Surface Measurements
SeaWiFS	Sea-viewing Wide Field-of-view Sensor
SO	Successive Orders of scattering code (RTC developed by LISE/UdL)
S/W	Sofware
SZA	Solar Zenith angle
TriOS	Tri-Optical Sensor (hyperspectral radiometer)
TOA	Top Of the Atmosphere
UT	Universal Time (or GMT, Greenwich Mean Time)
VAA	View Azimuthal angle
VZA	View Zenith angle
WP	Work Package

1.5.2. Scientific units

deg	degree (*angle unit*)
$D.U.$	Dobson Unit (*atmospheric ozone columnar density unit*) *(Note: 1 D.U. =0.001 cm-atm)*
hPa	hecto Pascal or 10^2 *Pa* (*pressure unit*) *(Note: 1 atm = 760.31 torr = 1013.25 hPa; 1 torr = 1mmHg = 1.333 mbar)*
$m.s^{-1}$	meter per second (*speed unit*)
μm	micrometer (*wavelength unit*)
nm	nanometer (*wavelength unit*)
$n.u.$	no unit (*or unitless*)
sr	steradian (*solid angle unit*)
$W.m^{-2}$	Watt per square meter (*radiant flux unit*)
$mW.m^{-2}.nm^{-1}$	milli-watt per square of meter per nanometer (*spectral irradiance unit*)
$mW.m^{-2}.nm^{-1}.sr^{-1}$	milli-watt per square of meter per nanometer per steradian (*spectral radiance unit*)

2. THE TRIOS PROCESSOR

Above water measurements with the TriOS field sensor consists in simultaneous acquisitions of the surface irradiance (E_d), the radiance emerging from sea water (L_w) which includes the contribution of the surface, and the downwelling atmospheric (or sky) radiance (L_{sky}) [AD-3]. The TriOS viewing geometry to collect these above water measurements is depicted on Figure 1.

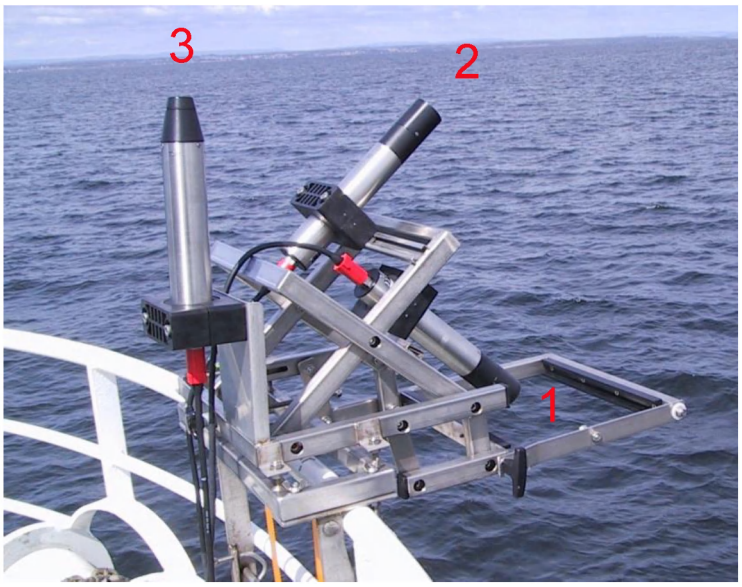

Figure 1: TriOS measurement geometry for (1) above water radiance (L_w), (2) downwelling sky radiance (L_{sky}), and (3) surface irradiance (E_d). The radiometric measurements are nominally acquired for VZA=40 deg. and RAA=135 deg.

2.1. The TriOS Input File

The next 8 tables hereafter display a sample of data sequence acquired in the Northern sea extracted from the TriOS measurement data file provided by the MUMM institude. It corresponds to the TriOS data acquisition on April 23th, 2003. From the date and the time (UT) of the data sequence acquisition and its associated geographic position in (*lat*, *long*), the Sun solar zenith angle (SZA) has then been computed. SZA is reported in this input SeaPRISM file as well the assumed fixed nominal TriOS viewing direction (VZA=40 *deg.*, RAA=135 *deg.*). This first block of information are given in Table 1.

Table 1: Geographical position (lat, long), date/time and Sun/view geometrical conditions for the selected radiometric data sequence acquired with the TriOS in the Northern sea.

lat_IS (*deg.*)	lon_IS (*deg.*)	time_IS (*UT*)	thetas_IS (*deg.*)	thetav_IS (*deg.*)	dphi_IS (*deg.*)
51.272	2.904	20030423T082400Z	56.2670	40.000	135.000

The following blocks of data consits in the TriOS radiometric measurements. TriOS being an hyperspectral resolution sensor (HRS) all the radiometric quantities are spectrally convoluted with the 13 MERIS filters, knowing that the 2 gaseous aborption bands centred at 762 *nm* and 900 *nm* have been discarded.

The first block of data corresponds to the in-situ surface irradiances (E_{d_IS}) in the 13 MERIS spectral bands (Table 2). This E_{d_IS} spectrum is plotted in Figure 2.

Table 2: Surface irradiances collected in the 13 MERIS spectral bands for the selected radiometric data sequence acquired with the TriOS in the Northern sea.

Ed_IS_412.5 ($mW/m^2/nm$)	Ed_IS_442.5 ($mW/m^2/nm$)	Ed_IS_490 ($mW/m^2/nm$)	Ed_IS_510 ($mW/m^2/nm$)	Ed_IS_560 ($mW/m^2/nm$)	Ed_IS_620 ($mW/m^2/nm$)
513.90570	595.73169	661.75916	652.47205	641.09918	596.51080

Ed_IS_665 ($mW/m^2/nm$)	Ed_IS_681.25 ($mW/m^2/nm$)	Ed_IS_708.75 ($mW/m^2/nm$)	Ed_IS_753.75 ($mW/m^2/nm$)	Ed_IS_778.75 ($mW/m^2/nm$)	Ed_IS_865 ($mW/m^2/nm$)	Ed_IS_885 ($mW/m^2/nm$)
583.17456	564.40692	535.75793	473.19101	472.57150	393.00830	380.98706

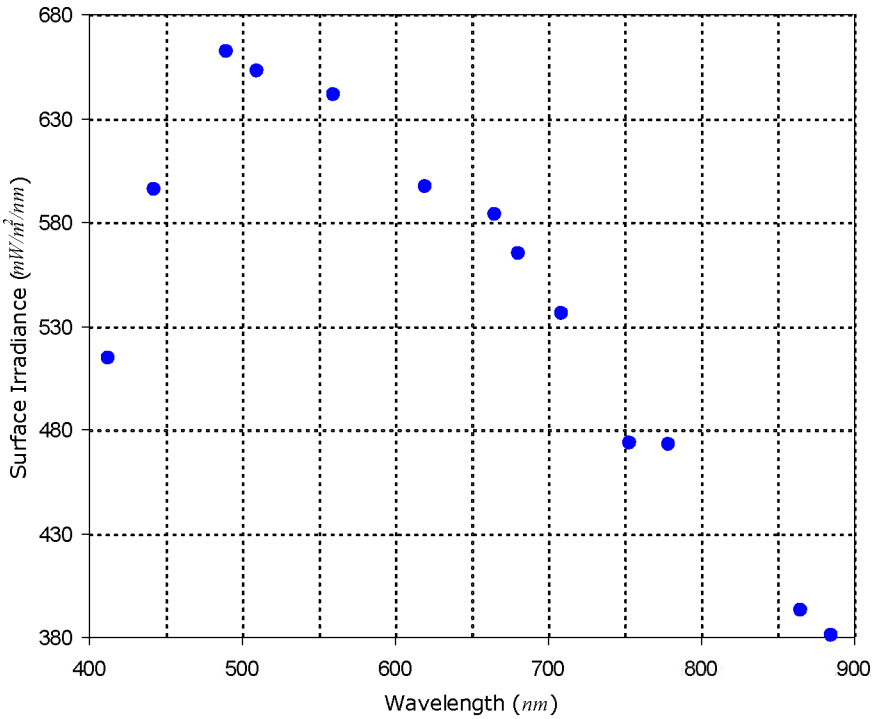

Figure 2: Surface irradiance (E_d) measurements in the 13 MERIS spectral bands (after applying a spectral convolution of TriOS E_d acquisitions with the MERIS filters).

The second block of data is the set of 13 in-situ water-leaving radiances (L_{w_IS}) corrected for the sky dome reflection, by removing the *Fresnel* reflection contribution of the sea surface to the above water radiance measurement (L_{se_IS}). This standard correction is achieved as:

$$L_{w\_IS}(\lambda,\theta,\phi) = L_{se\_IS}(\lambda,\theta,\phi) - R(\theta,\phi,\theta_o,w_s)\cdot L_{sky\_IS}(\lambda,\theta',\phi), \quad (1)$$

in which R represents the *Fresnel* reflection coefficient of the sea surface as a function of the Sun/view geometry (θ, ϕ, θ_o), and L_{sky_IS}, the downwelling sky radiance measurement (*see* Figure 1) and the level of surface roughess induced by the wind-speed (w_s). At a given fixed viewing geometry (*i.e.*, θ= 40 *deg.*, ϕ=90 *deg.*), R is estimated as a function of θ_o and w_s [RD-1][RD-3]. For our selected data sequence, these water-leaving radiances are displayed at the 13 MERIS spectral bands in Table 3.

Table 3: Water-leaving radiances ($mW/m^2/nm/sr$) corrected for the sky dome reflection with the standard protocol in the 13 MERIS spectral bands, for a given TriOS radiometric data sequence.

Lw_IS_412.5 ($mW/m^2/nm/sr$)	Lw_IS_442.5 ($mW/m^2/nm/sr$)	Lw_IS_490 ($mW/m^2/nm/sr$)	Lw_IS_510 ($mW/m^2/nm/sr$)	Lw_IS_560 ($mW/m^2/nm/sr$)	Lw_IS_620 ($mW/m^2/nm/sr$)
2.91785600	3.68011590	5.50485850	6.60049340	10.84472800	8.17169570

Lw_IS_665 ($mW/m^2/nm/sr$)	Lw_IS_681.25 ($mW/m^2/nm/sr$)	Lw_IS_708.75 ($mW/m^2/nm/sr$)	Lw_IS_753.75 ($mW/m^2/nm/sr$)	Lw_IS_778.75 ($mW/m^2/nm/sr$)	Lw_IS_865 ($mW/m^2/nm/sr$)	Lw_IS_885 ($mW/m^2/nm/sr$)
5.20097680	4.96837470	5.47526500	1.53846260	1.42812610	0.72672719	0.61574328

The next block of data represents the set of 13 in-situ sky radiance measurements (L_{sky_IS}), *i.e.* the atmospheric downwelling radiances at BOA for the 13 MERIS spectral bands (Table 4). L_{sky} is used for removing the contribution of the sky dome reflection from the above water radiance measurement (L_{se_IS}). The L_{sky_IS} spectrum is depicted on Figure 3.

Table 4: Sky radiances ($mW/m^2/nm/sr$) measured in the 13 MERIS spectral bands, for a given TriOS radiometric data sequence.

Lsky_IS_412.5 ($mW/m^2/nm/sr$)	Lsky_IS_442.5 ($mW/m^2/nm/sr$)	Lsky_IS_490 ($mW/m^2/nm/sr$)	Lsky_IS_510 ($mW/m^2/nm/sr$)	Lsky_IS_560 ($mW/m^2/nm/sr$)	Lsky_IS_620 ($mW/m^2/nm/sr$)
62.98400900	59.11538700	49.06905700	43.08190200	32.95424700	23.49524100

Lsky_IS_665 ($mW/m^2/nm/sr$)	Lsky_IS_681.25 ($mW/m^2/nm/sr$)	Lsky_IS_708.75 ($mW/m^2/nm/sr$)	Lsky_IS_753.75 ($mW/m^2/nm/sr$)	Lsky_IS_778.75 ($mW/m^2/nm/sr$)	Lsky_IS_865 ($mW/m^2/nm/sr$)	Lsky_IS_885 ($mW/m^2/nm/sr$)
19.21068000	17.48103900	15.16900100	11.53923700	10.83670900	7.30070260	6.73414610

As for the last block of data, the latter corresponds to the set of 13 in-situ above water radiance measurements (L_{se_IS}), *i.e.* the upwelling radiances mesured at BOA in the 13 MERIS spectral bands (Table 5). The plot of the L_{se_IS} spectrum is dsiplayed on Figure 3.

Table 5: Above water radiances ($mW/m^2/nm/sr$) measured in the 13 MERIS spectral bands, for a given TriOS radiometric data sequence.

Lse_IS_412.5 ($mW/m^2/nm/sr$)	Lse_IS_442.5 ($mW/m^2/nm/sr$)	Lse_IS_490 ($mW/m^2/nm/sr$)	Lse_IS_510 ($mW/m^2/nm/sr$)	Lse_IS_560 ($mW/m^2/nm/sr$)	Lse_IS_620 ($mW/m^2/nm/sr$)
4.70659400	5.35898690	6.89838030	7.82402900	11.78064000	8.83893970

Lse_IS_665 ($mW/m^2/nm/sr$)	Lse_IS_681.25 ($mW/m^2/nm/sr$)	Lse_IS_708.75 ($mW/m^2/nm/sr$)	Lse_IS_753.75 ($mW/m^2/nm/sr$)	Lse_IS_778.75 ($mW/m^2/nm/sr$)	Lse_IS_865 ($mW/m^2/nm/sr$)	Lse_IS_885 ($mW/m^2/nm/sr$)
5.74659440	5.46483520	5.90607260	1.86618550	1.73592090	0.93405491	0.80701238

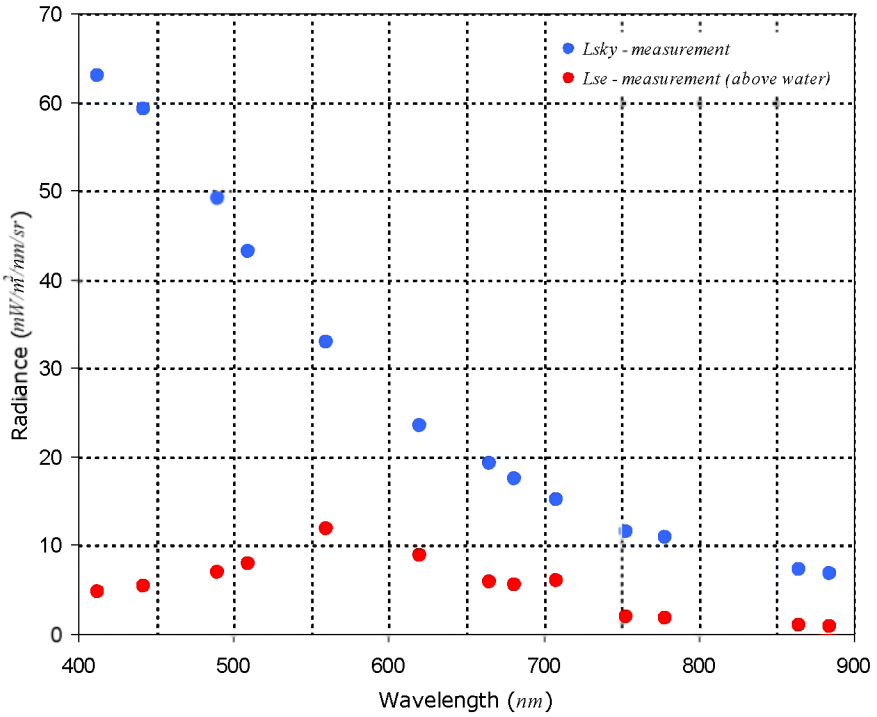

Figure 3: Sky radiance (L_{sky_IS}) and above water radiance measurements (L_{se_IS}) in the 13 MERIS spectral bands (after applying a spectral convolution of TriOS radiometric data with the MERIS filters).

At the end, some auxiliary data are provided in the input TriOS file (Table 6): the in-situ wind-speed ($wind_{IS}$) above sea level (m/s), the *Fresnel* reflection coefficient of the sea surface (R, denoted as $Fresnel_{IS}$) estimated with input w_s [RD-1][RD-3], and the in-situ surface pressure (hPa) from climatology.

Table 6: Auxiliary data associated with a given TriOS data sequence.

Wind_IS (m/s)	Fresnel_IS ($n.u.$)	Pressure_IS (hPa)
5.00	0.028400	1019.00

2.2. The MERMAID Input Data File

2.2.1. Extraction of relevant pieces of information

To compute the new *Fresnel* reflection coefficient (R_{pol}) of the sea surface, which accounts for polarization, both the informations about the wind-speed (w_s), and the aerosols are required. Morever, the computation of the BOA reflected Sun glint radiance needs, in addition to the in-situ ($wind_{IS}$), the atmospheric ozone content (u_{O3}) that will be included in the attenuation of the direct Sun glint radiance along the downwelling path. For these two computations, we use then the MERMAID data file generated with a window size of (5 x 5) pixels in the MERIS reduced resolution (RR) mode. For our sample of TriOS data sequence presented in Section 2.1, the associated relevant data for the wind-speed and the aerosols have been extracted from the MERMAID data file for the AAOT site (Table 7). We can note that both the wind-speed (w_s) and the ozone amount u_{O3}) slowly vary in the MERIS-RR window as the result of a bilinear interpolation on the ECMWF grid. The pair of standard aerosol models (*i.e.*, the 2 bracketing SAMs) may be very variable in the window. Note that R_{pol} will be computed for all the pixels where at least one of the bracketing aersosol assemblage corresponds to one of the 16 SAMs indexed from 0 to 12 (model#0, MAR, COA, RUR) and from 31 to 33 (BLU-IOPs).

Table 7: Extracted aerosol product, wind-speed (w_s) and total ozone amoumt (u_{O3}) from the MERMAID file at the AAOT site, associated with the selected SeaPRISM data sequence from Section 2.1. The aerosol parameters consists in the total AOT at 865 nm (AOT_865), the Angstroem exponent (alpha), the 2 bracketing SAMs (iaer1,iaer2) and the aerosol mixing rate (aer_mix).

AOT_865 (*n.u.*)	*alpha* (*n.u.*)	*iaer1* (*n.u.*)	*iaer2* (*n.u.*)	*aer_mix* (*n.u.*)	w_s (*m/s*)	u_{O3} (*Dobson*)
0.137816	1.970894	11	31	0.871669	4.344218	389.08687
0.162565	1.721611	11	31	0.378354	4.349443	389.04999
0.185802	1.546142	12	11	0.858180	4.354815	389.01312
0.185830	1.544682	12	11	0.851328	4.360333	388.97624
0.182995	1.566102	12	11	0.949722	4.365995	388.93937
0.191988	1.564387	12	11	0.944629	4.338581	389.04187
0.190529	1.568989	12	11	0.965137	4.343822	389.00624
0.190648	1.539367	12	11	0.827899	4.349210	388.97062
0.190675	1.537932	12	11	0.821110	4.354743	388.93499
0.193593	1.503975	12	11	0.657113	4.360422	388.89937
0.201493	1.533885	12	11	0.805697	4.332945	388.99687
0.204854	1.508549	12	11	0.684328	4.338202	388.96249
0.202446	1.492155	12	11	0.601489	4.343606	388.92812
0.202471	1.490803	12	11	0.594660	4.349156	388.89374
0.197868	1.502784	12	11	0.652933	4.354851	388.85937
0.215133	1.543495	12	11	0.855638	4.327312	388.95187
0.201520	1.562436	12	11	0.938645	4.332585	388.91874
0.201258	1.546117	12	11	0.863248	4.338004	388.88562
0.201281	1.544738	12	11	0.856815	4.343570	388.85249
0.202858	1.505183	12	11	0.666894	4.349282	388.81937

AOT_865 (*n.u.*)	*alpha* (*n.u.*)	*iaer1* (*n.u.*)	*iaer2* (*n.u.*)	*aer_mix* (*n.u.*)	w_s (*m/s*)	u_{O3} (*Dobson*)
0.413176	1.260641	5	12	0.738220	4.321680	388.90687
0.212016	1.562196	12	11	0.940756	4.326969	388.87499
0.213405	1.507180	12	11	0.680982	4.332404	388.84312
0.213426	1.505877	12	11	0.674568	4.337986	388.81124
0.203093	1.539291	12	11	0.831849	4.343714	388.77937

2.2.2. Range definition of relevant parameters

In order to define the range values of each relevant parameter, an analysis of the full MERMAID database has been conducted regardless of the Northern sea area where the TriOS measurements were acquired. The results are presented and fully discussed in [AD-4]. They are summarized as follows:

- The range of SZA has been selected as [0;75] deg.
- The range of w_s has been defined as [0;20] $m.s^{-1}$ and an extrapolation will be used for the values below 1.5 $m.s^{-1}$ as well as above 10 $m.s^{-1}$.
- The barometric pressure, for all the MERMAID database collected at sea level, varies very few around the standard pressure (P_o=1013.25 hPa). The latter, which does not impact much on the *Fresnel* reflection coefficient, is then assumed to be fixed to this standard value as done in the POLREF simulator.

2.3. Determination of the Atmospheric Model

For the molecules, the *Rayleigh* optical thickness (ROT, referred also as to τ_R) is derived from the *Hansen and Travis* formulation [RD-4], for a standard barometric pressure (P_s) of 1013.25 hPa. Table 8 displays the ROT values at the 13 MERIS nominal wavelengths.

Table 8: Rayleigh optical thickness in each of the 13 MERIS spectral bands.

λ	*412.50*	*442.50*	*490.00*	*510.00*	*560.00*	*620.00*	*665.00*
τ_R	0.315280	0.235910	0.155155	0.131714	0.089912	0.059433	0.044730

λ	*681.25*	*708.75*	*753.75*	*761.875*	*778.75*	*865.00*	*885.00*	*900.00*
τ_R	0.040562	0.034558	0.026944	0.025802	0.023617	0.015459	0.014099	0.013176

As for the ozone optical thickness (OOT), the latter is computed from the total ozone amount (u_{O3}), expressed as *cm-atm*. This calculation is completed by appling u_{O3} as a weighting factor to the tabulated values (τ_{O3}) given for a reference amount of 1 *cm-atm* within the 13 MERIS filters (Table 9).

Table 9: Ozone optical thickness (τ_{O3}) in each of the 13 MERIS spectral bands for an amount (u_{O3}) of 1 cm-atm. These values are extracted from the MERIS level-2 ADFs used in the 3rd MERIS reprocessing.

λ	412.50	442.50	490.00	510.00	560.00
τ_{O3}	2.17850600 10^{-4}	2.81364330 10^{-3}	2.00568866 10^{-2}	4.08085547 10^{-2}	1.03985801 10^{-1}

λ	620.00	665.00	681.25	708.75	753.75
τ_{O3}	1.09030262 10^{-1}	5.05040102 10^{-2}	3.52579132 10^{-2}	1.88077260 10^{-2}	8.89660790 10^{-3}

λ	761.875	778.75	865.00	885.00	900.00
τ_{O3}	6.63424140 10^{-3}	7.69330280 10^{-3}	2.19219110 10^{-3}	1.21072340 10^{-3}	1.51665860 10^{-3}

For the aerosols, a particular treatment of the mixing layer (Figure 4) is activated in the "*atmosphere*" routine in order to get the total AOT at the 13 MERIS wavelengths. The block of inputs is related to the MERIS aerosol product. These aerosol parameters, defined for the whole atmosphere, consist in the 2 bracketing assemblages (*iaer1*, *iaer2*), the mixing rate (*aermix*), the AOT at 865 *nm* (*AOT865*) and the *Angstroem* exponent, $\alpha(779,865)$. The processing of the mixing-layer is fully detailed in Annex-2 from [AD-4].

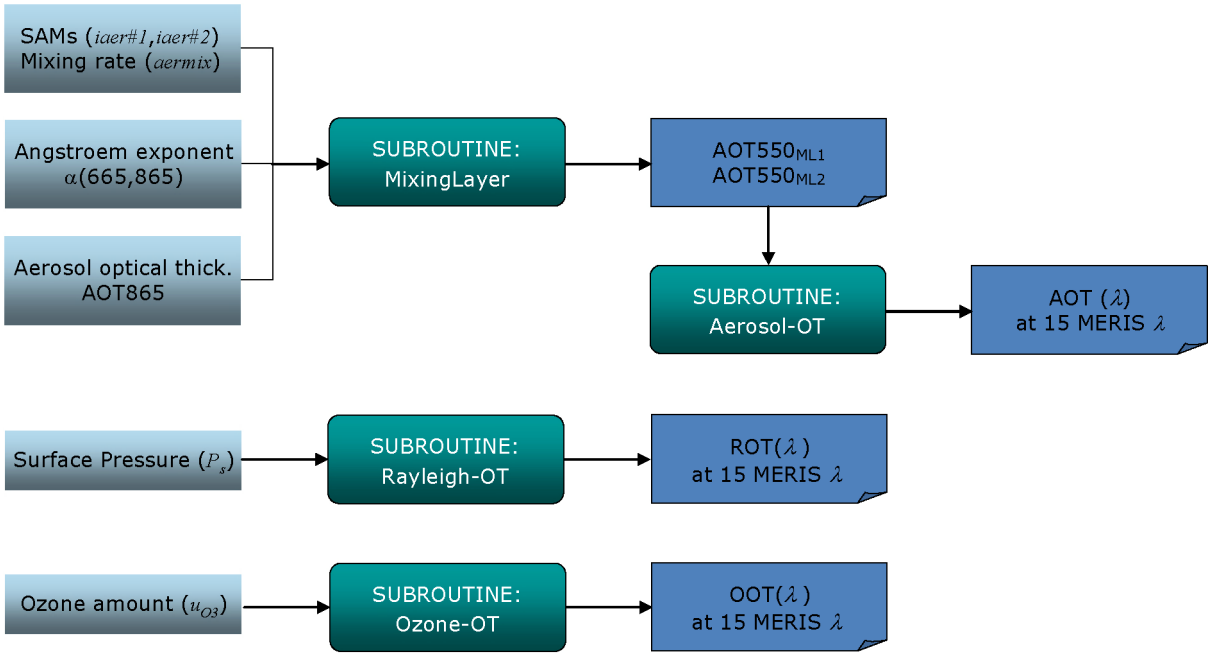

Figure 4: Flow chart of the "atmosphere" routine to get the total optical thickness in the 15 MERIS spectral bands. It includes a 1st tool to extract the AOT550 in the mixing layer for each of the 2 bracketing SAMs, to recombine them and to get the total AOT at the 15 MERIS wavelengths, and 2 additional tools to get ROT and OOT at the 15 MERIS wavelengths.

The outputs from the "*atmosphere*" routine are first, the AOT, ROT and OOT at the 15 MERIS wavelengths, for the attenuation of the direct Sun glint radiance at BOA (Section 2.4). Second, this

routine provides the AOT550 in the mixing layer associated with each of the 2 bracketing SAMs, for the computation of the *Fresnel* reflection coefficient (Section 2.5).

The above computation is looped on the 25 pixels from the MERIS-RR window. When the aerosol product is undefined, then $iaer1$ and $iaer2$ will be set to *-999*. If the aerosol product exists, then both the 2 bracketing SAMs ($iaer1$, $iaer2$) will be checked if they belong to the set of 16 SAMs used for generating for the SEAPOL database. In the MERIS aerosol classification, the standard *Fern and Shettle* assemblages are indexed ($iaer$) from 0 to 12 [RD-5], and the so-called BLU-IOP models from 31 to 33 [RD-6]. If one of the 2 bracketing assemblages is identified as a SAM then it will be kept as the unique assemblage for the next steps of the processing detailed in Sections 2.4 & 2.5. If both the 2 bracketing assemblages do not correspond to a SAM then the processing will be stopped and both the BOA reflected Sun glint radiance (L_{glint}, Section 2.4) and the new *Fresnel* reflection coefficient (R_{pol}, Section 2.5) will be set to -999.

In this report, we mainly focuse on the water-leaving radiance (L_{w_IS}). Having in mind that the sky radiance measurement (L_{sky_IS}) contains the coupling between the atmospheric scattering and the *Fresnel* reflection of the sea surface, the direct Sun glint radiance reflected at BOA (L_{glint}) has to be removed as well as the sky dome reflection contribution, from the upwelling above water radiance (L_{se_IS}) acquired in the TriOS field-of-view (FOV):

$$L_{w\_IS} = L_{se\_IS} - L_{gl\,\mathrm{int}} - R \cdot L_{sky\_IS} \qquad (2)$$

For MERIS, the Sun glint reflectance has been computed by assuming that the wind-roughened sea surface is modelled by a *Cox-Munk* wave-slope distribution driven by a wind-speed [RD-7]. At a given wavelength (λ), the direct attenuation of the solar beam along the Sun path is computed with the *Rayleigh* optical thickness weighted by the barometric pressure, the aerosol optical thickness extracted from the MERIS level-2 "Ocean-Aerosol" product and the ozone optical thickneyss which has been weighted by its total amount in the atmosphere.

2.4. Computation of the Sun Glint at BOA

2.4.1. Extraterrestrial spectral solar irradiance

The POLREF simulator developed for WP-1 [AD-1], returns as output a normalized radiance computed for a solar constant (F_o) of 1 $W.m^{-2}.\mu m^{-1}.sr^{-1}$ at top of the atmosphere (TOA). The conversion into the TriOS radiances requires firstly, to get the extraterrestrial solar spectral irradiances in the 13 MERIS spectral bands (excluding the O2 and H2O strong absorbing bands), and secondly a corrective factor to account for the temporal variation of the *Sun-Earth* distance. Using a spectrometric database of solar spectral irradiances [RD-8], the solar spectral constant can be estimated for the set of 13 MERIS nominal wavelengths using a spectral linear interpolation.

Table 10 lists this set of 13 MERIS F_o values. From the date/time of the TriOS data sequence acquisition is determined the *Julian* day (J),

$$J = day + (hh/24) + (mm/60) + (ss/3660), \quad (3)$$

with hh, mm, *and* ss respectively the *hour*, *minute* and *second* extracted from the time of the data sequence acquisition, and day the number of the day in the year computed as,

$$day = 31\,(month - 1) + dd + \eta, \quad (4)$$

with dd the day of the data sequence acquisition, and η defined as:

$$\begin{cases} \eta = 0, \; if \;\; month \le 2 \\ \eta = \left[(2 - month)/2 \right] - 2, \; if \;\; month > 8 \\ \eta = \left[(1 - month)/2 \right] - 2, \; elsewhere \end{cases}$$

The *Sun-Earth* distance (d_J), expressed as $A.U.$, is then estimated as:

$$d_J = A - B \cdot \cos(\gamma_J \cdot \pi/180) - \varepsilon \cdot \cos(\gamma_J \cdot \pi/90) \quad \text{with} \;\; \gamma_J = C \cdot J - D, \quad (5)$$

with, $\varepsilon = 0.00014$, $A = 1 + \varepsilon$, $B = 0.01671$, $C = 0.985600283$ and $D = 3.4532868$.

The extraterrestrial spectral solar irradiance (E_0^J) at the *Julian* day (J) is then corrected as:

$$E_0^J = F_o / d_J^2 \quad (6)$$

Table 10: Extraterrestrial spectral solar irradiances (F_o) computed at the 13 MERIS nominal wavelengths with a spectrometric database of the solar spectrum [RD-8].

$\lambda\,(nm)$	*412.50*	*442.50*	*490.00*	*510.00*	*560.00*	*620.00*	*665.00*
F_o $(mW/m^2/nm)$	171.476733	187.889294	192.833716	192.893628	180.307630	165.077380	153.162646

$\lambda\,(nm)$	*681.25*	*708.75*	*753.75*	*778.75*	*865.00*	*885.00*
F_o $(mW/m^2/nm)$	147.216809	140.794263	126.604285	117.725952	95.838519	92.983801

We have to keep in mind that the best practise to get the solar irradiances at TOA in each of the 13 MERIS band, should correspond to a spectral convolution of values from the spectrometric data-base with the spectral response of each MERIS filter.

However, from our point of view, because first the direct Sun glint reflected at BOA remains a residual term, and secondly, due to the uncertainties on the wind-speed value and on the wave-slope distribution model, then the approximation on the solar spectral irradiance is negligible.

2.4.2. Methodology

Both in the TriOS data file provided by the MUMM institute and in the MERMAID extraction file, all the information needed to calculate the direct Sun glint contribution at BOA in the field sensor spectral bands are available:

- date and time (UT) of data acquisition, to compute the *Julian* day useful to correct the extraterrestrial solar spectral irradiance for the *Sun-Earth* distance (Table 1),
- Sun solar zenith angles of data acquisition (Table 1),
- in-situ wind-speed above sea level (Table 6),
- aerosol, molecular and ozone optical thicknesses in the 13 MERIS spectral bands (Section 2.3).

The approach is illustrated in the general flow chart of the TriOS processor from Figure 5. In a first step, the direct Sun glint radiance will be calculated from the first three bullets in absence of atmosphere (L_{glint}). The *Cox-Munk* wave-slope distribution will be associated with the input wind-speed value from the MERMAID input data file to achieve this computation. The second step will consist in the attenuation of the direct Sun glint radiance along the downwelling atmospheric path. Then the latter will be reflected in the ground-based sensor direction through the *Fresnel* reflection coefficient at the air-sea interface. Finally, in a last step this reflected Sun glint radiance at BOA will be subtracted from the above water radiance measurement (L_{se_IS}).

This methodology is applied to each of the 25 pxiels in the MERIS RR-windows.

2.4.3. Statistics on L_{glint} in the MERIS-RR window

The removal of the skydome reflection contribution at BOA to each above water radiance measurement for a TriOS data sequence, needs to compute the statistics on the BOA reflected Sun glint radiance (L_{glint}) for the pixels within the MERIS-RR window. Mean and standard deviation values on L_{glint} (respectively, $<L_{glint}>$ and $\sigma_{L_{glint}}$) are then calculated for all the pixels for which the aerosol product is well defined and at least one of the bracketing aerosol assemblage correspond to a SAM. In other words, the pixel for which L_{glint} is set to -999 will be discarded from the computation of these statistics.

$<L_{glint}>$ will be then used to correct the water-leaving radiance measurement (L_{se_IS}) for the BOA reflected Sun glint (Eq.2).

2.5. Computation of Fresnel Reflection Coefficient (R_{pol})

2.5.1. MERIS BOA-atmospheric LUTs

In order to feed the TriOS processor, the MERIS BOA atmospheric LUTs have been extracted for a fixed viewing geometry (VZA~40 $deg.$) from the SEAPOL database generated upstream (*see* [AD-1] for more details).

Thus, for each of the 16 SAMs and each of the 3 wind-speeds (1.5, 5.0 and 10 $m.s^{-1}$) one binary LUT is provided including:

- BOA upwelling normalized radiances, $L_{boa}^{\uparrow}(\lambda, \tau_a^{550}, \mu_s, \Delta\phi)$,
- BOA downwelling normalized radiances, $L_{boa}^{\downarrow}(\lambda, \tau_a^{550}, \mu_s, \Delta\phi)$,
- Total downwelling atmospheric transmittances, $T_{tot}(\lambda, \tau_a^{550}, \mu_s)$ (referred as L_{boa_dw}),

computed for:

(*i*) an extraterrestrial solar irradiance (F_o) of π $W.m^{-2}.\mu m^{-1}.sr^{-1}$,
(*ii*) a standard surface pressure (P_s) of 1013.25 hPa,
(*iii*) a black water body,
(*iv*) a set of 25 SZAs (*i.e.*, θ_s values corresponding to 24 *Gaussian* angles + zenith direction), ranged from 0 to 88.14 $deg.$,
(*v*) a set of 25 RAAs $(\Delta\phi)$ regularly spaced (with a step of 7.5 $deg.$), ranged from 0 to 180 $deg.$, knowing that for the SeaPRISM data acquisitions RAA=90 $deg.$,
(*vi*) a set of 17 AOT at 550 nm (τ_a^{550}) for the boundary (or mixing) layer, including the pure molecular case and regularly spaced (with a step of 0.05), ranged from 0 to 0.8,
(*vii*) a set of 15 MERIS nominal wavelengths (λ).

Moreover, the BOA upward/downward radiances and transmittances are stored in the LUT with respect to the increasing values of its parameters (*i.e.*, $\lambda, \tau_a^{550}, \theta_s$ and $\Delta\phi$). For each SAM, 3 binary LUTs are associated with the 3 wind-speeds, the size of each being (15 x 17 x 25 x 25) single float precision, *i.e.*, 30.4 Mbytes for the full database of MERIS BOA atmospheric LUTs.

2.5.2. R_{pol} computation for each individual MERIS-RR pixel

The POLREF simulator [AD-1] represents the basement on which has been developed the TriOS processor. The general flow chart of the TriOS processor to compute both the BOA reflected Sun glint radiances and the *Fresnel* reflection coefficients at the 13 MERIS wavelengths, for each MERIS-RR pixel is depicted on Figure 5. This flow chart remains very close to the SeaPRISM's one presented in [AD-4], except that for SeaPRISM the direct Sun glint radiance at BOA is attenuated along the downwelling atmospheric path with a total optical thickness derived from in-situ measurements (AOT, ROT and OOT), while for the TriOS processor the direct Sun glint attenuation at BOA is computed with AOT, ROT and OOT from Section 2.3.

The main input used from the TriOS data file is the solar zenith angle (SZA). The other inputs come from the MERIS level-2 Ocean-Aerosol product (stored in the MERMAID data file).

Moreover, it has to be noticed that we do not need to account for the gaseous aborption in the calculation of R_{pol}.

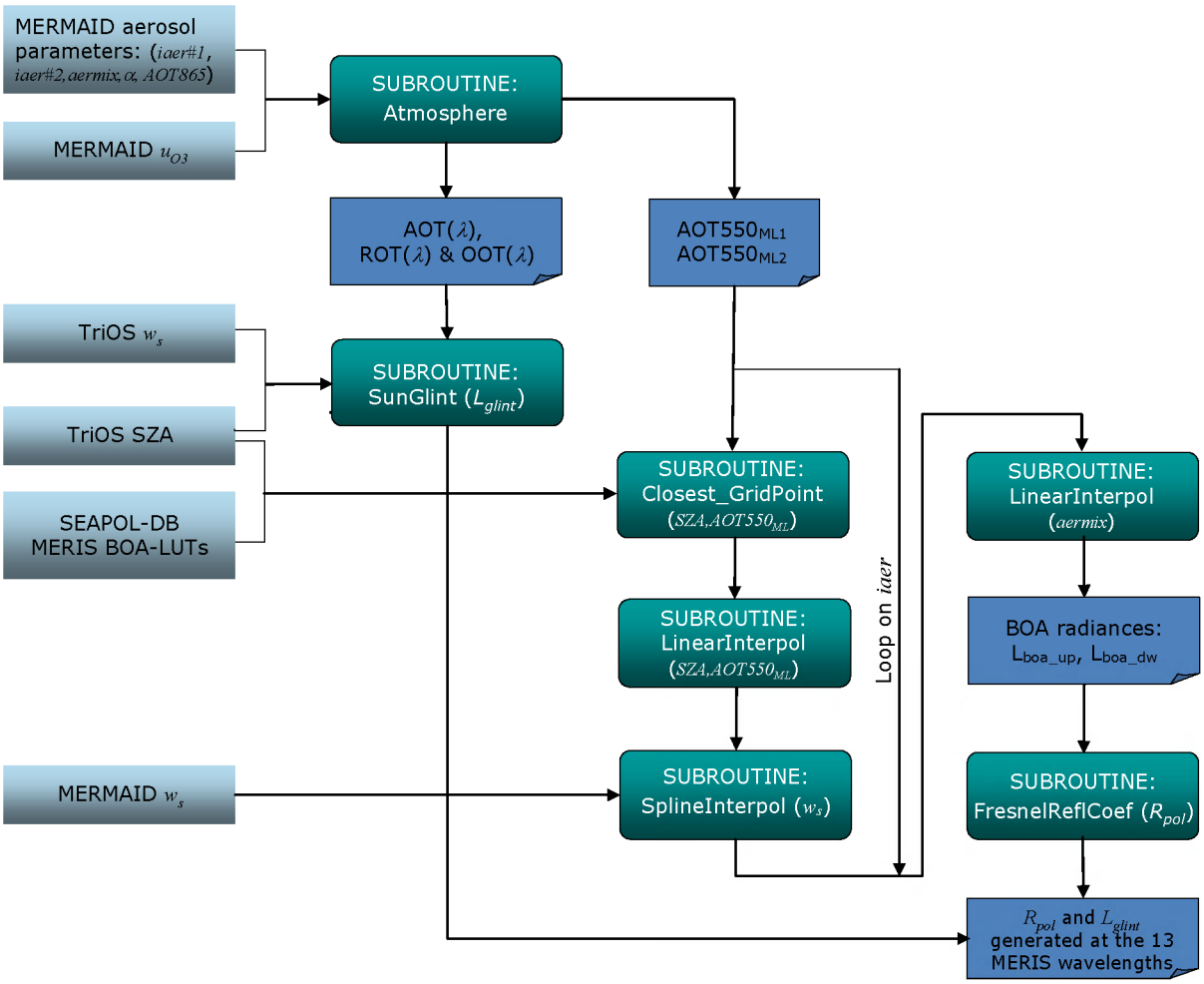

Figure 5: General flow chart of the TriOS processor to compute the Fresnel reflection coefficients (R_{pol}) and the BOA reflected Sun glint radiances in the 13 MERIS spectral bands.

The general flow chart of the TriOS processor is described by the following steps:

- Step-1: A first block of inputs is related to the MERMAID aerosol and ozone data file. These aerosol parameters and the ozone amount are then used to compute the atmospheric optical thickness (AOT + ROT + OOT) at the 13 MERIS wavelengths and the AOT at 550 *nm* ($AOT550_{ML1}$, $AOT550_{ML2}$) in the mixing layer for each of the 2 bracketing SAMs ($iaer1$, $iaer2$) as illustrated in Section 2.3. Note that the total AOT is computed as the sum of AOT contributions for the mixing layer and the upper atmospheric layers (*i.e.*, troposphere and stratosphere). Each of these inputs are previously checked upstream to be ranged within its validity domain. If one of them is out of range, then the process will be broken and R_{pol} and L_{glint} will be set to -999.

- Step-2: When at least one of the 2 bracketing assemblages is a SAM then the process continues to identify the aerosol composition in the mixing layer. For a given type of aerosol, the LUTs generation is driven by the AOT550 in the mixing layer ($AOT550_{ML}$). The approach to derive this information are fully detailed in Annex-1 from [AD-4].

For the case where both the 2 $AOT550_{ML}$ values corresponding to the 2 bracketing SAMs are retrieved as negative values, then the process will be stopped and R_{pol} and L_{glint} will be set to -999. If one of the 2 $AOT550_{ML}$ is retrieved as a positive value and the other one as a negative value, then the SAM associated with the positive $AOT550_{ML}$ will be kept as the unique assemblage to continue with the next steps of processing.

- Step-3: The input TriOS SZA value combined with $AOT550_{ML}$ extracted from Step-2 for a given bracketing SAM (*iaer1* or *iaer2*) are then employed as input in the "*Closest_GridPoint*" subroutine to look for the closest grid points by lower value in SZA, and AOT550 used in the MERIS BOA atmospheric LUTs. A multi-linear interpolation is then applied to get interpolated MERIS BOA upwelling/downwelling radiances at the input angular geometry (SZA, VZA=40 $deg.$, RAA=135 $deg.$) and extracted AOT550 ($AOT550_{ML}$) associated with the given bracketing SAM (*iaer1* or *iaer2*), at the 15 MERIS wavelengths and for each of the 3 tabulated wind-speeds (1.5, 5.0 & 10 $m.s^{-1}$). The "*LinearInterpol* (*SZA*,$AOT550_{ML}$)" subroutine is perfectly in line with the interpolation schemes implemented in the MERIS-IPF [AD-5].
- Step-4: Using the wind-speed (w_s) extracted from the input MERMAID data file, a cubic spline interpolation in wind-speed is then employed to get the MERIS BOA upward/downward radiances for w_s. This step is achieved for a given bracketing SAM (*iaer1* or *iaer2*) with the "*SplineInterpol* (w_s)" subroutine.
- Step-5: The previous 2 steps (Step-3 & Step-4) are completed again with the 2nd bracketing SAM (*iaer2*) if the latter exists and differs from the 1st one.
- Step-6: In the case where the 2 bracketing SAMs (*iaer1* and *iaer2*) differ, a final mixing recombination of individual contributions of the 2 SAMs is achieved with the "*LinearInterpol* (*aermix*)" subroutine, to get the final BOA upward/downward radiances at the 13 MERIS wavelengths.
- Step-7: The new *Fresnel* reflection coefficients (R_{pol}) of the sea surface are then computed at the 13 MERIS wavelengths with the "*FresnelReflCoef*(R_{pol})" subroutine.
- Step-8: The BOA reflected Sun glint radiances (L_{glint}) are calculated at the 13 MERIS wavelengths, with the methodology presented in Section 2.4.2, by using the TriOS SZA, the TriOS $wind_{IS}$, and the AOT, ROT & OOT from Step-1, as inputs to the "*SunGlint*(L_{glint})" subroutine.

Some remarks:

(i) When the 2 bracketing SAMs differ, the resulting $AOT550_{ML}$ in the boundary layer is computed as a simple linear combination of the aerosol mixing (*aermix*):

$$AOT550_{ML} = AOT550_{ML1} \cdot (1 - aermix) + AOT550_{ML2} \cdot aermix \quad (7)$$

The total AOT at each of the 13MERIS wavelength is then deduced from the IOPs of the aerosols in the boundary layer, troposphere and stratosphere (*see* [AD-6] for more details).

(*ii*) The negative retrieval of the $AOT550_{ML}$ from Step-2 should have to be deeply investigated in the future in regards to the MERIS DPM [AD-5].

(*iii*) The cubic spline interpolation in wind-speed from Step-4, is justified by the analysis of the wind-speed influence on the radiance presented in [AD-4]. It clearly appears that the w_s-dependence of the radiance can be modelled by a 2nd or 3rd order polynomial fit.

2.5.3. Statistics on R_{pol} and L_{glint} in the MERIS-RR window

The general flow chart presented in Section 2.5.2 applies to each pixel of the MERIS-RR window (*i.e.*, 5 x 5 pixels). In order to correct the water-leaving radiances from a given TriOS data sequence, the average and the standard deviation (*i*) on the *Fresnel* reflection coefficient (respectively, $<R_{pol}>$ and $\sigma_{R_{pol}}$) and (*ii*) one the BOA reflected Sun glint radiance (respectively, $<L_{glint}>$ and $\sigma_{L_{glint}}$) are computed with the individual R_{pol} or L_{glint} values of pixels in the MERIS-RR window. Pixels for which R_{pol} or L_{glint} is undefined (set to -999) will be discarded from the computation of these statistics.

$<R_{pol}>$ and $<L_{glint}>$ will be used to correct the water-leaving radiance measurement (L_{w_IS}) for the sky dome reflection by using Eq.2.

2.5.4. Processing of the full TriOS data archive

In order to process the full TriOS database on an operational basis, a loop on the data sequences has been included in the TriOS processor S/W. Both the input TriOS data file and the MERMAID input data file will have to write in a sequential mode by addding datalines corresponding to the input TriOS data sequences, and its associated block of (5 x 5) datalines corresponding to the aerosol parameters, the wind-speed and the ozone amount of each of the 25 pixels in the MERIS-RR windows. Moreover, all the empty data fields for which the aerosol product is undefined will have to be set by a default value equal to -999.

2.6. The TriOS Output File

The new TriOS file provided by the processor is formatted as the input TriOS file. The latter includes a new set of water-leaving radiances at the 13 MERIS wavelengths corrected for both the BOA reflected Sun glint contribution and the sky dome reflection (Table 11). The Sun glint and sky dome corrections are achieved with Eq.2 by using $<L_{glint}>$ as estimated in Section 2.4 and $<R_{pol}>$ as defined in Section 2.5.

Table 11: New water-leaving radiances ($mW/m^2/nm/sr$) corrected for both the BOA reflected direct Sun glint and the sky dome reflection with R_{pol} computed by the processor, at the 13 MERIS nominal wavelengths, for the given original radiometric data sequence acquired with the TriOS in the Northern sea.

Lw_IS_412.5 ($mW/m^2/nm/sr$)	Lw_IS_442.5 ($mW/m^2/nm/sr$)	Lw_IS_490 ($mW/m^2/nm/sr$)	Lw_IS_510 ($mW/m^2/nm/sr$)	Lw_IS_560 ($mW/m^2/nm/sr$)	Lw_IS_620 ($mW/m^2/nm/sr$)
2.79249296	3.53747867	5.36896992	6.47453064	10.74743274	8.09493047

Lw_IS_665 ($mW/m^2/nm/sr$)	Lw_IS_681.25 ($mW/m^2/nm/sr$)	Lw_IS_708.75 ($mW/m^2/nm/sr$)	Lw_IS_753.75 ($mW/m^2/nm/sr$)	Lw_IS_778.75 ($mW/m^2/nm/sr$)	Lw_IS_865 ($mW/m^2/nm/sr$)	Lw_IS_885 ($mW/m^2/nm/sr$)
5.13423188	4.90567742	5.41800726	1.49082520	1.38221668	0.69380368	0.58509748

In order to conduct a quality control of the outputs produced by the TriOS processor, additional parameters are added as followings:

- the number of pixel from the MERIS-RR window for which R_{pol} is well defined (Table 12),
- the set of mean values of the *Fresnel* reflection coefficient $<R_{pol}>$ computed at the 13 MERIS wavelengths (Table 12),
- the set of standard deviation values of the *Fresnel* reflection coefficients ($\sigma_{R_{pol}}$) computed at the 13 MERIS wavelengths (Table 13),
- the set of mean values of the BOA reflected Sun glint radiances $<L_{glint}>$ computed at the 13 MERIS wavelengths (Table 14),
- the set of standard deviation values of the BOA reflected Sun glint radiances $<L_{glint}>$ computed at the 13 MERIS wavelengths (Table 15).

Table 12: New set of mean values of Fresnel reflection coefficients computed with the TriOS processor at the 13 MERIS wavelengths, for the given original radiometric data sequence acquired with the TriOS in the Northern sea.

npixel (*n.u.*)	Rpol_Mean_412.5 (*n.u.*)	Rpol_Mean_442.5 (*n.u.*)	Rpol_Mean_490 (*n.u.*)	Rpol_Mean_510 (*n.u.*)	Rpol_Mean_560 (*n.u.*)	Rpol_Mean_620 (*n.u.*)
25	0.03039027	0.03081276	0.03116853	0.03132402	0.03135278	0.03166638

Rpol_Mean_665 (*n.u.*)	Rpol_Mean_681.25 (*n.u.*)	Rpol_Mean_708.75 (*n.u.*)	Rpol_Mean_753.75 (*n.u.*)	Rpol_Mean_778.75 (*n.u.*)	Rpol_Mean_865 (*n.u.*)	Rpol_Mean_885 (*n.u.*)
0.03187615	0.03198653	0.03217518	0.03252904	0.03263945	0.03290796	0.03295368

Table 13: New set of standard deviation values of Fresnel reflection coefficients computed with the TriOS processor at the 13 MERIS wavelengths, for the given original radiometric data sequence acquired with the TriOS in the Northern sea.

Rpol_Stdev_412.5 (*n.u.*)	Rpol_Stdev_442.5 (*n.u.*)	Rpol_Stdev_490 (*n.u.*)	Rpol_Stdev_510 (*n.u.*)	Rpol_Stdev_560 (*n.u.*)	Rpol_Stdev_620 (*n.u.*)
0.00023608	0.00025451	0.00025616	0.00025062	0.00026838	0.00034101

Rpol_Stdev_665 (*n.u.*)	Rpol_Stdev_681.25 (*n.u.*)	Rpol_Stdev_708.75 (*n.u.*)	Rpol_Stdev_753.75 (*n.u.*)	Rpol_Stdev_778.75 (*n.u.*)	Rpol_Stdev_865 (*n.u.*)	Rpol_Stdev_885 (*n.u.*)
0.00035109	0.00035842	0.00036835	0.00032298	0.00031221	0.00037413	0.00036758

Table 14: Set of mean values of BOA reflected direct Sun glint computed with the TriOS processor at the 13 MERIS wavelengths, for the given original radiometric data sequence acquired with the TriOS in the Northern sea.

Lglt_Mean_412.5 (*mW/m²/nm/sr*)	Lglt_Mean_442.5 (*mW/m²/nm/sr*)	Lglt_Mean_490 (*mW/m²/nm/sr*)	Lglt_Mean_510 (*mW/m²/nm/sr*)	Lglt_Mean_560 (*mW/m²/nm/sr*)	Lglt_Mean_620 (*mW/m²/nm/sr*)
0.00000000	0.00000000	0.00000000	0.00000000	0.00000000	0.00000000

Lglt_Mean_665 (*mW/m²/nm/sr*)	Lglt_Mean_681.25 (*mW/m²/nm/sr*)	Lglt_Mean_708.75 (*mW/m²/nm/sr*)	Lglt_Mean_753.75 (*mW/m²/nm/sr*)	Lglt_Mean_778.75 (*mW/m²/nm/sr*)	Lglt_Mean_865 (*mW/m²/nm/sr*)	Lglt_Mean_885 (*mW/m²/nm/sr*)
0.00000000	0.00000000	0.00000000	0.00000000	0.00000000	0.00000000	0.00000000

Table 15: Set of standard deviation values of BOA reflected direct Sun glint computed with the TriOS processor at the 13 MERIS wavelengths, for the given original radiometric data sequence acquired with the TriOS in the Northern sea.

Lglt_Stdev412.5 (*mW/m²/nm/sr*)	Lglt_Stdev442.5 (*mW/m²/nm/sr*)	Lglt_Stdev490 (*mW/m²/nm/sr*)	Lglt_Stdev510 (*mW/m²/nm/sr*)	Lglt_Stdev560 (*mW/m²/nm/sr*)	Lglt_Stdev620 (*mW/m²/nm/sr*)
0.00000000	0.00000000	0.00000000	0.00000000	0.00000000	0.00000000

Lglt_Stdev665 (*mW/m²/nm/sr*)	Lglt_Stdev681.25 (*mW/m²/nm/sr*)	Lglt_Stdev708.75 (*mW/m²/nm/sr*)	Lglt_Stdev753.75 (*mW/m²/nm/sr*)	Lglt_Stdev778.75 (*mW/m²/nm/sr*)	Lglt_Stdev865 (*mW/m²/nm/sr*)	Lglt_Stdev885 (*mW/m²/nm/sr*)
0.00000000	0.00000000	0.00000000	0.00000000	0.00000000	0.00000000	0.00000000

Figure 6 displays the new *Fresnel* reflection coefficient $<R_{pol}>$ computed with the TriOS processor at the 13 MERIS wavelengths, for the selected data sequence acquired over the Northern sea on April 23th, 2003 at 08:24am (UT). Error bars have been reported on this plot to illustrate the dispersion on R_{pol} within the MERIS-RR window of (5 x 5) pixels. Compared with the R value estimated with the polynomial fit function of (SZA, w_s) from the standard protocol [RD-3], the new *Fresnel* reflection coefficient $<R_{pol}>$ is greater whatever the wavelength, stressing the importance to account for the polarization in both the sea surface reflection and the atmospheric scattering.

The water-leaving radiances (L_{w_IS}) corrected for the sky dome reflection with the standard protocol (*Mobley*) and with the TriOS processor are depicted on Figure 7. As expected for this given Sun/view geometry (SZA=56 *deg.*, VZA=40 *deg.*, RAA=135 *deg.*), compared with the standard protocol the sky dome reflection contribution is overestimated with the TriOS processor and the new water-leaving radiance is lower than the *Mobley*'s one, whatever the MERIS wavelength. As

plotted in Figure 8, these deviations can reach up to 5% in relative percentage differences (RPD) between the standard protocol and the TriOS processor.

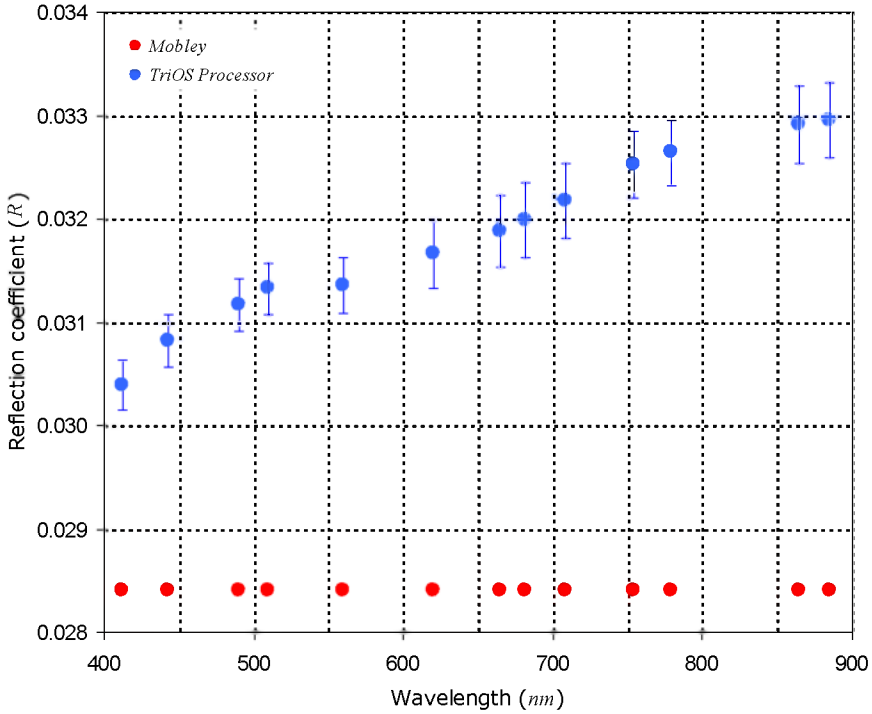

Figure 6: Comparison of the Fresnel reflection coefficients (R) estimated with the standard protocol (Mobley) and computed with the TriOS processor in a window of (5 x 5) pixels, at the 13 MERIS wavelengths and for a given TriOS data sequence acquired on April 23th, 2003 (08:24am) in the Northern sea. Vertical bars are associated with the standard deviation (±σ) around the mean value of R_{pol} for the window of (5 x 5) pixels.

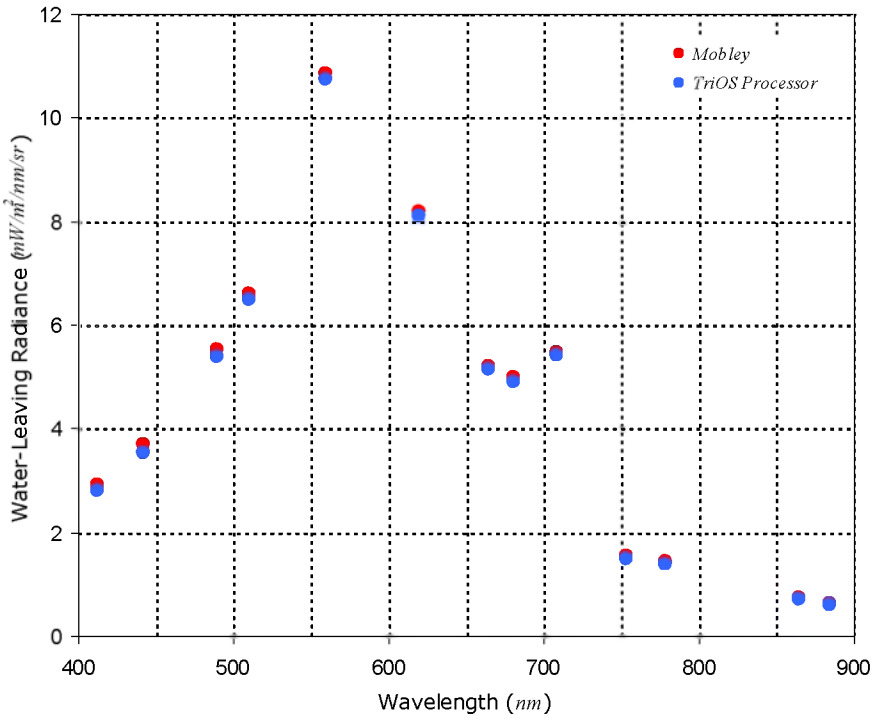

Figure 7: Water-leaving radiances corrected for the sky dome reflection using the standard protocol (Mobley) and the TriOS processor at the 13 MERIS wavelengths, for a given TriOS data sequence acquired on April 23th, 2003 (8:24am) in the Northern sea.

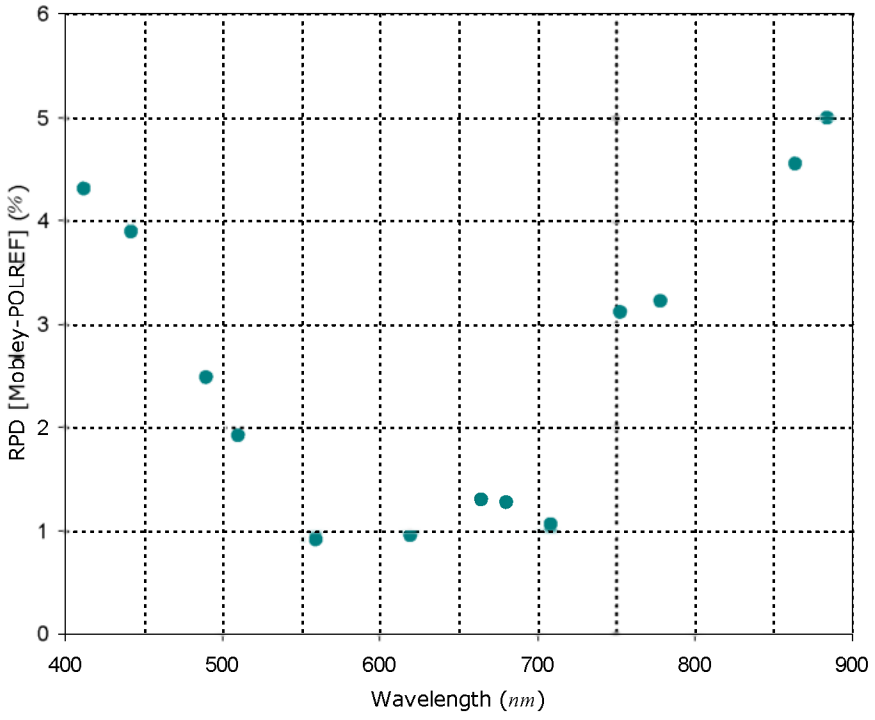

Figure 8: Relative percentage difference in water-leaving radiances corrected for the sky dome reflection, between the standard protocol (Mobley) and the TriOS processor, for the 13 MERIS wavelengths and a given TriOS data sequence acquired on April 23th, 2003 (8:24am) in the Northern sea.

3. PERSPECTIVES

The software package with the TriOS processor has been delivered to ARGANS on March 9th 2012. ARGANS is in charge to implement this new tool in the MERMAID in-situ data processing chain, and to produce the new set of water-leaving radiance measurements corrected for both the reflected Sun glint contribution at BOA and the sky dome reflection. ARGANS will process the in-situ databases for the 2 or 3 available databases acquired over the Northern sea by the MUMM institute. These new MERMAID files (including the new *Fresnel* reflection coefficients and the BOA reflected Sun glint radiances) will be analyzed as soon as ARGANS will deliver them to ADRINORD.

The TriOS aboard the Ferrybox (commercial ship) represents a major database with radiometric above water measurements in the Baltic sea. The main difference with the TriOS used by the MUMM institute is that the relative azimuth angle between the Sun/view directions varies. The latter will be then considered as an additional input. Keeping a fixed direction in view zenith angle (VZA), three sets of MERIS BOA LUTs will have to be associated with three VZAs (15 $deg.$, 40 $deg.$ and 55 $deg.$). More, because of the Sun/view geometry in the above water radiometric data acquisition, it is firstly important to correct for the Sun glint contribution at BOA, and secondly to flag in case where the correction is too high compared with the water body reflectance.

For the MERIS matchup, the aerosol assemblage is well known, but as for the SeaPRISM [AD-4], it is quite important to process all the available measurements in order to get an extensive database of in-situ water reflectances. This requires to get information about the aerosols. The inversion of the aerosol model as described in [RD-9] should be implemented and validated.

– END OF DOCUMENT –